

## Studies on Photo Luminescence Spectra of Certain rare earth ions Doped Alkali Borotellurite Glasses

P.Suryanagi Reddy<sup>1</sup>, Dr P.Saraswathi<sup>2</sup>, B.Vani Sree<sup>3</sup> Dr N.Vijaya laksmi<sup>4</sup>

1. Associate professor of physics S.S.B.N. Degree College, Anantapur.AP.India

2. Asst.professor of physics, S.D.G.S.College, Hindupur.AP. India

3. Asst.professor of chemistry. , S.D.G.S.College, Hindupur.AP. India

4 Asst.professor of physics .Govt degree college.kukat palli. TS.India.

Corresponding author: P.Suryanagi Reddy

Date of Submission: 30-08-2020

Date of Acceptance: 08-09-2020

**ABSTRACT:** The basic theory which deals with the various physical and the spectroscopic properties of lanthanide activated materials. It has been useful in understanding the lasing efficiencies of the non-crystalline materials towards the progress of the existing awareness in the glass technology. These results describe the formation and property characterization of the  $\text{Ho}^{3+}$  doped borotellurite glasses. This study gives a detailed analysis on the absorption, have been evaluated for all the glasses are studied. The applicability of Judd – Unfelt theory in understanding the absorption and emission properties of rare earth doped glasses has been verified by combining the absorption spectra computed parametric data with that of measured emission data. In the present study an attempt is made to find out wave lengths and densities of glasses and to bring out the formulation of the new series of high quality optical materials and the study carried out the different properties concerning physical, Luminance spectra of the rare earth ion  $\text{Ho}^{3+}$  doped borotellurite glasses.

**KEY WORDS:** MODEL F-3010 Spectro photometer.  $\text{H}_3\text{BO}_3$ ,  $\text{TeO}_2$ ,  $\text{BaCO}_3$ ,  $\text{Li}_2\text{CO}_3$ ,  $\text{NaCO}_3$ ,  $\text{NaCO}_3$ ,  $\text{SmF}_3$ ,  $\text{DyF}_3$  and  $\text{EuF}_3$

### I. INTRODUCTION:

According to American Society for Testing Materials (ASTM) “glass is an inorganic product of fusion which has been cooled to a rigid condition without crystallizing”. The glasses found in nature represent molten rock masses, which were extruded and cooled so quickly that they did not have time to become transformed into the usual aggregate of crystalline minerals. The commonest of these natural glasses, obsidian is usually translucent and blackish in color but it is

sometimes red, Brown or greenish and some varieties are transparent. It is easily broken into sharp, often elongated pieces, which lend themselves readily to the fashioning of arrow heads, spearheads and knives. Borosilicate glass for laboratory apparatus (Pyrex) is a twentieth century invention. Galileo’s work on the motion of the planets with the astronomical telescopes needing glass lenses. Isaac Newton’s pioneering work in optics begun in 1666. Other basic investigations which required glass apparatus were the classic investigations of the properties of gases (Boyle’s law and Charles’s law) thermometry, barometry and the development of microscopes. The inorganic non-oxide glasses such as the chalcogenides sharing many general structural similarities with oxides quite unexpected inorganic systems of which the halide, especially fluoride, glasses are the most notable metallic glasses and organic glasses, X- ray diffraction analysis of crystal structures was a particularly exciting field, which had an enormous impact on glass science. Glasses now play an increasingly important role in modern technology. Besides common glass, which is indispensable material in today’s economy in architecture, transport, lighting, condition etc., there is a whole set of glasses which enter into more and more sophisticated applications in optics, electronics and opto-electronics, biotechnologies and so on.

**II. EXPERIMENTAL PROCEDURE:**

**Preparation of Glass:** The following are the nine-borotellurite glasses prepared for their spectral analysis.

**TABLE (1)**

Glass type	Composition (Mol%)	UV Transmission	IR Transmission
Glass A	65B <sub>2</sub> O <sub>3</sub> +2TeO <sub>2</sub> +10BaO+22Li <sub>2</sub> O+1REF <sub>3</sub>	350 nm	4.5 μm
Glass B	65B <sub>2</sub> O <sub>3</sub> +2TeO <sub>2</sub> +10BaO+22Na <sub>2</sub> O+1REF <sub>3</sub>	360nm	4.3 μm
Glass C	65B <sub>2</sub> O <sub>3</sub> +2TeO <sub>2</sub> +10BaO+22K <sub>2</sub> O+ 1REF <sub>3</sub> (RE = Ho <sup>3+</sup> )	360nm	4.4 μm

For convenience the glasses have been labeled as Glass A, B, and C respectively. All the chemicals used in the present work were of analytical grade in 99.99% purity. The elements that used were spectrally pure (H<sub>3</sub>BO<sub>3</sub>, TeO<sub>2</sub>, BaCO<sub>3</sub>, Li<sub>2</sub>CO<sub>3</sub>, NaCO<sub>3</sub>, SmF<sub>3</sub>, DyF<sub>3</sub> and EuF<sub>3</sub>). The rare-earths were purchased from M/S Indian rare-earth Ltd; Udyogmandal, Kerala state and the chemical TeO<sub>2</sub> (99.995 % Purity) was purchased from M/S Aldrich, Toronto, Canada and other chemicals from a local chemical firm. Each of the above batches (8 gm in weight) was collected into an agate mortar to crush them as finer powder for homogeneous mixing. Every time the mortar and the pestle were cleaned properly. The powdered chemicals were collected into silica (or) porcelain crucibles for melting in an electric furnace (900-950° C).

The melts were sand – witted between two smooth surfaced plates for obtaining the glass samples in circular designs with 1-2 cm in diameter and with thickness of 0.25 cm. These glasses were prepared by adopting quenching technique [1-5].

The determination of refractive indices (n<sub>d</sub>) at 589.3 nm and densities of these glasses were carried out and the results are given below.

**TABLE (2)**

Glass type	n <sub>d</sub> (λ589.3 nm)	D (gm <sup>-3</sup> )
Glass A	1.5656	2.106
Glass B	1.5846	2.199
Glass C	1.5125	2.145

The above table clearly describes the dependence of the refractive index and density values both on the changes made in the alkali content and also on the rare earth ions present in the glass systems examined.

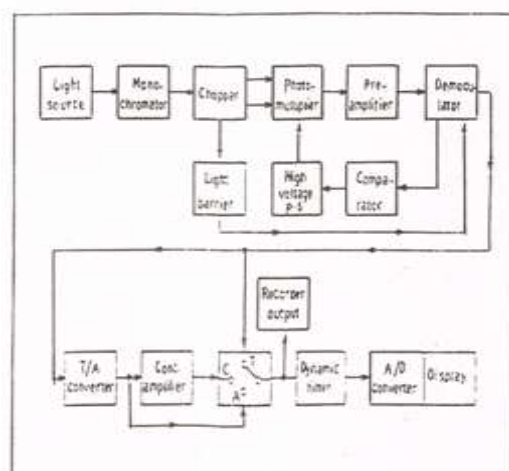
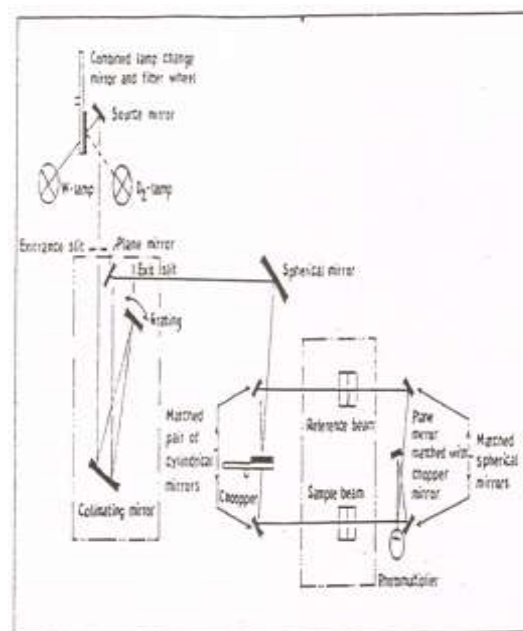


FIG.1: PERKIN-ELMER-551 RECORDING SPECTROPHOTOMETER (Block diagram)



OUTLINE OF INSTRUMENT

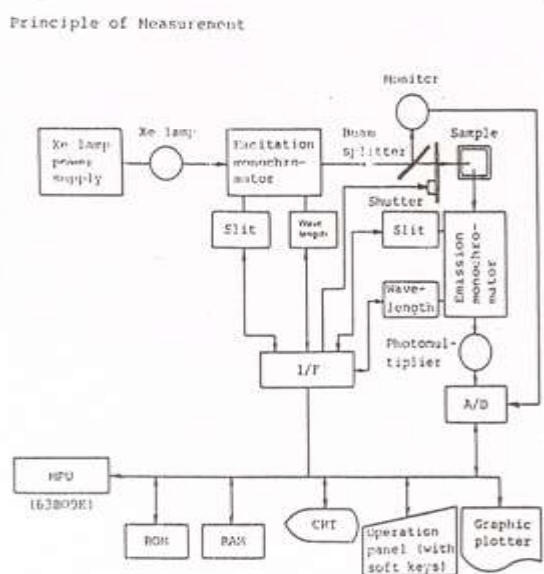


Fig. 3 : Functional block diagram of the Model F-3010

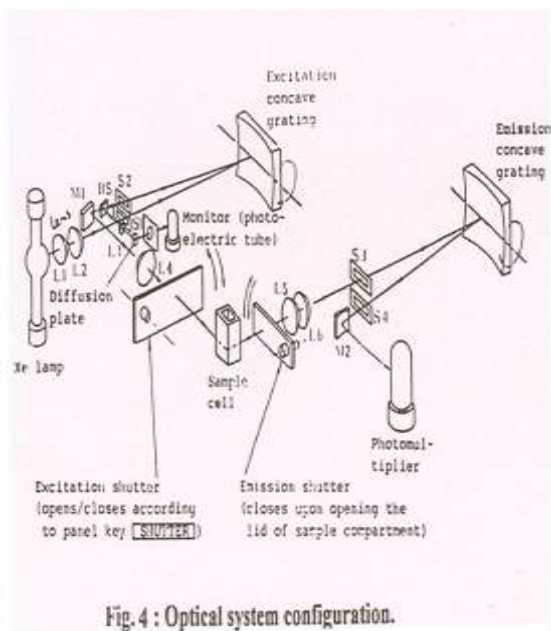


Fig. 4 : Optical system configuration.

**Spectral measurements:**

**Photoluminescence spectra:** Luminescence is a term to describe the radioactive combination of carriers (electrons and holes) excited by a variety of methods light (Photoluminescence), High energy electrons (cathodoluminescence) or an electric field (electroluminescence). The term fluorescence is generally reserved for those radioactive transitions

for which the emitted photon energy is different (generally lower) from the energy of excitation. The energy difference arises because of appreciable non-radioactive energy loss suppressed by the excited carriers until the radioactive recombination occurs.

Both excitation and Photoluminescence spectra were carried out on a Hitachi F-3010 spectrofluorimeter. We had access to this facility at Central Instrumentation Laboratory, University of Hyderabad, India. The experimental setup used for fluorescence recording is shown in fig.3. And optical alignment is presented in Fig.4.

The Wavelength range for the glass is  
 $Ho^{3+}$  -----450—600 nm ----- (1)

The wavelengths (nm) of the spectral features were converted into their wave numbers ( $cm^{-1}$ ) by using the wave number tables available in the literature [6-8].

To analyze the Photoluminescence spectra of the rare-earth materials, it is necessary to apply the Judd-Ofelt results obtained from the absorption measurements of these optical of florescence levels and to calculate the Judd-Ofelt parameters ( $\Omega_2$ ), the radiative properties of florescence levels could be determined in the direction of such radiative property estimation, firstly, the electric dipole line strengths  $S_{ed} (\Psi^1 J^1 \rightarrow \Psi J)$  of the emission levels are to be evaluated. To determine the  $S_{ed}$  values of the emission levels, the required squared metric elements  $\|U_2\|^2$  of various excited states ( $\Psi^1 J^1 \rightarrow \Psi J$ ) of  $Ln^{3+}$  doped materials given in literature [39-42] are used. These matrix elements are not changing significantly depending on the glass matrix environments. Therefore, the same results reported by these authors are used in present work as well. However, for reference purpose, the energies ( $\nu$ ) and the squared reduced matrix elements  $\|U_2\|^2$  used in the work are tabulated in Tables 3,5 & 7 for the difference states of  $Sm^{3+}$ ;  $Dy^{3+}$  and  $Eu^{3+}$  respectively. The spontaneous emission probability for an electronics dipole transition dipole transition is obtained

$$A(S^1 L^1 J^1 \rightarrow S L J) = \frac{64 \pi^4 \nu^3 e^3}{3h(2J+1)} \frac{1}{n(n^2+2)^2} S_{ed} \quad 9$$

Where  $\gamma$  = emission energy level ( $Cm^{-1}$ )  
 $h$  = Planck's constant  
 $n_d$  = the refractive index of the material.

The relaxation rate (total transition probability from an initial manifold ( $S^1 L^1 J^1$ ) to a final (SLJ) is written as

$$A_T(S^1L^1J^1) = \sum A(S^1L^1J^1:SLJ)$$

$$S^1L^1J^1$$

The fluorescence branching ration ( $\beta^1J^1J$ ) for transition  $A(S^1L^1J^1:SLJ)$

$$A(S^1L^1J^1:SLJ)$$

$$\beta^1J^1J = \frac{A(S^1L^1J^1:SLJ)}{\sum A(S^1L^1J^1:SLJ)}$$

$$A_T(S^1L^1J^1)$$

Where the sum runs over all the possible terminal manifolds.

Finally, the stimulated emission cross-sections for the measured fluorescence levels are to be calculated

$$\sigma_p^E = \frac{\lambda_p^4 A(S^1L^1J^1:SLJ)}{8 \pi c n_d^2 \Delta \lambda_p}$$

Where  $\lambda_p$  corresponds to the peak position of the emission line and  $\Delta \lambda_p$  is an effective band – width which is used because of the symmetry of the emission lines and is obtained by dividing the integrated emission band by the intensity at  $\lambda_p$ . The values  $\sigma_p^E$  will be in magnitudes of  $10^{-20} - 10^{-22} \text{ cm}^2$

A diagram describing the relationship between the absorption and photoluminescence spectra of rare – earths doped materials has been shown in Fig.1. A combination of experimental photoluminescence results and Judd-Ofelt analysis of the absorption data enables to determine a set of radiative properties, which allows the selection of suitable laser host materials. This approach thus helps us to tailor the glass systems in efficiencies.

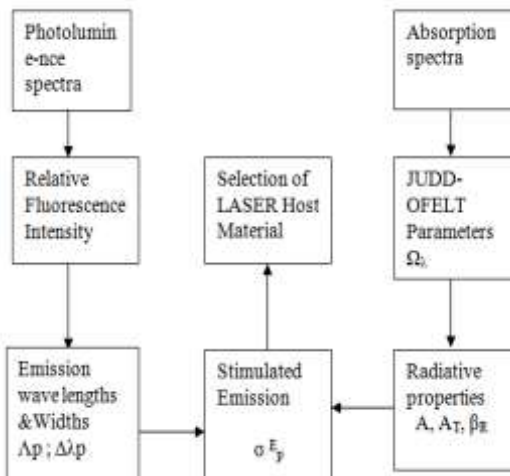
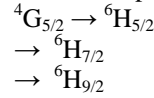


Fig. 5. Relationship between the absorption and the photoluminescence spectral results in the Selection of laser host material.

**Photoluminescence Properties:** The following are the emission spectral profiles were observed for the  $\text{Ho}^{3+}$  doped glasses.



The spectral profiles are given in the figs. 1.(d)-(f).

The values of transition probabilities  $A(s^1)$ , total transition probabilities  $A_T(s^1)$  and radiative life time laser transitions ( $T_r$ ), electric dipole line strengths ( $S_{ed}$ ) and branching ratios  $\beta_R$  % for  $\text{Ho}^{3+}$  doped glasses are presented in Table. 1(b). The values of relaxation rates  $A_T$  are found to be greater in glass ‘A’ compared to glass B and C.

The stimulated emission cross sections ( $\sigma_p^E$ ) have been evaluated from the expression.

$$\sigma_p^E = \frac{\lambda_p^4 A}{8 \pi c n_d^2 \Delta \lambda}$$

Where  $\lambda_p$  is the peak fluorescence wavelength (nm) of emission band and  $\Delta \lambda$  is the Fluorescence band width by integrating the fluorescence line shape and dividing by the intensity at  $\lambda_p$ . ‘c’ is the velocity of light, ‘ $n_d$ ’ is the refractive of glass and ‘A’ is the transmission probability of the emission level. The measured values of emission wavelengths ( $\lambda_p$ ) and bandwidths ( $\Delta \lambda$ ) and stimulated emission cross sections ( $\sigma_p$ ) of  $\text{Ho}^{3+}$  doped glasses are summarized in Table.

**Table.3.**

Emission level energies ( $\gamma \text{ cm}^{-1}$ ) and squared reduced matrix elements  $\|U^\lambda\|^2$  ( $\lambda = 2,4,6$ ) For different bands of  $\text{Sm}^{3+}$  [17]

Transition	Energy ( $\gamma \text{ cm}^{-1}$ )	$\ U^2\ ^2$	$\ U^4\ ^2$	$\ U^6\ ^2$
$^4G_{5/2} \rightarrow ^6F_{11/2}$	7448	0	0	0
$\rightarrow ^6F_{9/2}$	8842	0.0016	0.0002	0.0002
$\rightarrow ^6F_{7/2}$	10022	0	0.0015	0.0015
$\rightarrow ^6F_{5/2}$	10800	0.0062	0.0014	0
$\rightarrow ^6F_{3/2}$	11394	0.0010	0	0
$\rightarrow ^6H_{5/2}$	11511	0	0	0
$\rightarrow ^6F_{13/2}$	11644	0	0	0
$\rightarrow ^6H_{11/2}$	12959	0	0	0.0014
$\rightarrow ^6H_{9/2}$	14364	0	0.0045	0.0018
$\rightarrow ^6H_{7/2}$	15690	0.0096	0.0061	0.0019
$\rightarrow ^6H_{5/2}$	16896	0	0.0078	0.0075
$\rightarrow ^6H_{5/2}$	17930	0.0002	0.0007	0

**Table.4.**

Emission level energies ( $\gamma \text{ cm}^{-1}$ ) and squared reduced matrix elements  $\|U^\lambda\|^2$  ( $\lambda = 2,4,6$ )

For different bands of  $\text{Sm}^{3+}$  [22]

Transition	Energy( $\gamma \text{ cm}^{-1}$ )	$\ U^2\ $ $\  \quad \ ^2$	$\ U^4\ $ $\  \quad \ ^2$	$\ U^6\ $ $\  \quad \ ^2$
$^4F_{9/2} \rightarrow$	7414	0	0	0
$^6F_{1/2}$	7961	0	0	0
$\rightarrow ^6F_{3/2}$	8757	0.0062	0.0008	0.0004
$\rightarrow ^6F_{5/2}$	10158	0.0002	0.0043	0.0029
$\rightarrow ^6F_{7/2}$	10955	0	0.0035	0.0011
$\rightarrow ^6H_{5/2}$	12005	0.0008	0.0079	0.0067
$\rightarrow ^6H_{7/2}$	12062	0.0007	0.0055	0.0004
$\rightarrow ^6F_{9/2}$	13375	0.0032	0.0032	0.0024
$\rightarrow ^6F_{11/2}$	13422	0.0021	0.0024	0.0032
$\rightarrow ^6H_{9/2}$	15276	0.0093	0.0018	0.0033
$\rightarrow ^6H_{11/2}$	17602	0.0490	0.064	0.545
$\rightarrow ^6H_{13/2}$	21053	0	0.0046	0.0292
$\rightarrow ^6H_{15/2}$				

**Table.5.**

Emission level energies ( $\gamma \text{ cm}^{-1}$ ) and squared reduced matrix elements  $\|U^\lambda\|^2$  ( $\lambda = 2,4,6$ )

For different bands of  $\text{Eu}^{3+}$  [22]

Transition	Energy ( $\gamma \text{ cm}^{-1}$ )	$\ U^2\ $ $\  \quad \ ^2$	$\ U^4\ $ $\  \quad \ ^2$	$\ U^6\ $ $\  \quad \ ^2$
$^5D_0 \rightarrow ^7F$		0.0000	0.0000	0.0002
$^6_7F_4$	12386	0.0000	0.0020	0.0000
$^7F_2$		0.0028	0.0000	0.0000
$^5D_1 \rightarrow ^7F$	14470	0.0000	0.0000	0.0003
$^6_7F_5$		0.0000	0.0006	0.0000
$^7F_4$	16267	0.0000	0.0024	0.0000
$^7F_3$	13997	0.0033	0.0016	0.0000
$^7F_2$		0.0007	0.0000	0.0000
$^7F_1$	15099	0.0023	0.0000	0.0000
	16160			
	17146			
	18008			
	18676			

**III. RESULTS AND DISCUSSIONS:**

**Holmium doped glasses as laser glasses:** There has been one demonstration [8] of  $\text{Ho}^{3+}$  doped waveguide laser that employed a silica fiber co-doped with Germania. Laser emission due to the  $^4G_{5/2} \rightarrow ^6H_{9/2}$  transition at 651 nm was excited by an argon laser at 488 nm. The fluorescence peak caused by this transition is relatively narrow at only

3.3 nm, suggesting that only a single pair of stark levels is involved. In fact the fluorescence spectrum of  $\text{Ho}^{3+}$  in high – silica glass has considerable fine structure [9] suggesting that inhomogeneous broadening of the energy levels is not severe. The detestable level does, however, exhibit a non exponential decay with a life time of 1.7 ms. This long life time, the four-level nature of the system, and large stimulated cross section due to the narrowness of the prospect of an efficient, low- threshold, Q- switched fiber laser [9]. Although the lasing properties of this ion have not been used in a ZBLAN waveguide, the fluorescence spectrum [10] is also finely structured, suggesting that in this host glass  $\text{Ho}^{3+}$  will exhibit similarly attractive properties. In addition the branching ratio is slightly different, indication that other visible transitions may also be made to laser. The determination of refractive indices ( $n_d$ ) at 589.3 nm and densities of these glasses were carried out and the results are given below.

**TABLE (6)**

Glass type	$n_d$ ( $\lambda 589.3$ nm)	D ( $\text{gm}^{-3}$ )
Glass A	1.5656	2.106
Glass B	1.5846	2.199
Glass C	1.5125	2.145

The above table clearly describes the dependence of the refractive index and density values both on the changes made in the alkali content and also on the rare earth ions present in the glass systems examined. fig(1),fig (2) and fig (3) shows the graphs of Absorption spectra of Glass A, Glass B, and Glass C .

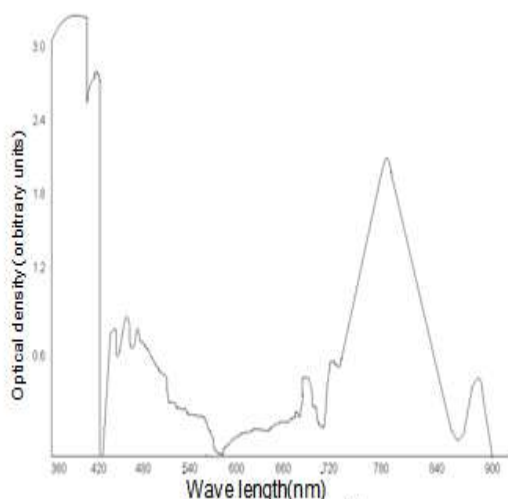


Fig. 1.(a): Absorption Spectra of  $\text{Ho}^{3+}$  doped Glass A

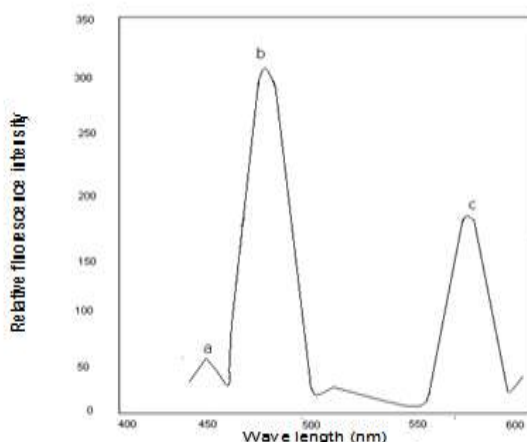


Fig 1.(e). Photoluminescence Spectrum of  $\text{Ho}^{3+}$  doped glass B

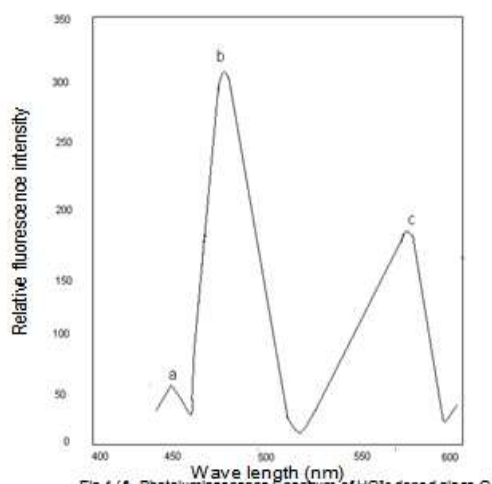


Fig 1.(f). Photoluminescence Spectrum of  $\text{Ho}^{3+}$  doped glass C

**REFERENCES:**

- [1]. C.D.Coleman, W.R. Bozman and W.F. Meggers. Tables of Wave numbers [National Bureau of Standards, Washington D.C., 1960]
- [2]. A. Pual Chemistry of glasses, Chapman & Hall, London (1983)
- [3]. S.V.J.Lakshman and S.Srinivas, Wave number Tables (2000-900  $\text{A}^\circ$ ) Maruti Book Depot. Guntur, India (1988)
- [4]. S.V.J.Lakshman, Problems in spectroscopy, COSTED, Madras, India (1988)
- [5]. G. Amernath, S.Buddhudu, F.J.Bryant, XiLuo, B.Yu and S.Huang J.Lumin. 47 (1991) 255
- [6]. K. Annapurna, and J.V.Sathyanarayana, S.Buddhudu and a.Mandelis J. Alloys & Comp. 216 (1994) 281
- [7]. K.Annapurna and S.Buddhudu, J.Phys. D: Appl. Phys. 26 (1993) 302
- [8]. J.V.Sathyanarayana, K.Annapurna and S. Buddhudu, Mater. Res. Bull. 29 (1994) 1263
- [9]. M.A.Saltzberg and H.H.Yung, J.Amer. Ceram. Soc. 73 (1990) 2897
- [10]. Tammann, G, Der Glaszustand Leipzig: L.3 (1933)
- [11]. J.Sugar, Phys. Rev.Lett. 14 (1965) 731
- [12]. M.I. Weber, RA. Saroyan and R.C.Ropp, J. Non-Cryst. Solids, 44 (1981) 137.